ELSEVIER

Journal of Power Sources 83 (1999) 50–56

JOURNAL OF POWER SOURCES

www.elsevier.com/locate/jpowsour

Properties of a new type of cathode for molten carbonate fuel cells

Seung Taek Kuk, Young Seck Song, Keon Kim *

Department of Chemistry, Korea University, 1, Anam-dong, Sungbuk-Ku, Seoul, 132-701, South Korea

Received 27 January 1999; accepted 3 March 1999

Abstract

The solubility of a nickel oxide cathode in molten carbonate fuel cell (MCFC) electrolyte is one of the major technical obstacles to the commercialization of such fuel cells. Lithium cobalt oxide, $LiCoO_2$, has been selected as a candidate material for MCFC cathodes because its solubility is small and the rate of dissolution into the melt is slower than that for nickel oxide. On the other hand, the electrical conductivity of $LiCoO_2$ is lower than that of nickel oxide. Thus, nickel oxide has been coated with stable $LiCoO_2$ in carbonate by a PVA-assisted sol–gel method to give a $LiCoO_2$-coated NiO (LC-NiO) cathode. Raman spectra show that the structure of LC-NiO is different from that of nickel oxide, and that a $LiCo_{1-y}Ni_yO_2$ phase is formed during heat-treatment of the LC-NiO cathode. The coating of $LiCoO_2$ on NiO electrode increases with increase in the dipping and heating times. The performance of unit cells show that the mean voltage of the cells is 0.80 V using a NiO cathode and 0.85 V with a LC-NiO cathode at a current density of 150 mA cm^{-2}. The solubility of the LC-NiO cathode in molten carbonate electrolyte is half that of NiO cathode after 300 h at 650°C.

Keywords: Fuel cell; Lithium cobalt oxide; $LiCoO_2$-coated NiO cathode; PVA-assisted sol–gel

1. Introduction

The molten carbonate fuel cell (MCFC) is expected to be an efficient device for the conversion of chemical energy in the near future [1–3]. Research and development on MCFCs have been performed in several countries and many researchers have made vigorous efforts to improve cell performance and life. A typical fuel cell consists of a porous nickel anode and a porous nickel oxide cathode. These electrodes are separated by an electrolyte structure, or tile, which is comprised of a mixture of molten alkali metal carbonates retained by capillary action in the interstices of an array of chemically inert inorganic crystallites. One of the major limits to the lifetime of a MCFC is the dissolution of the nickel oxide cathode in the electrolyte [4,5]. There is also a risk that dissolved nickel will precipitate in the matrix on the anode side and cause short-circuiting of the cell. This problem can be overcome by two possible ways. One is to adjust the composition of the carbonates to retard dissolution of nickel oxide and the other is to find an alternative material to replace nickel oxide. In recent years, a large effort has been directed to the development of alternative cathode materials [5–7]. Lithium cobalt oxide, $LiCoO_2$, is a candidate material because the solubility is small and the rate of dissolution is slower than that of NiO. Although the electronic conductivity of $LiCoO_2$ is lower than that of NiO, it can be increased by improved preparation methods [8].

Pechini [9] invented a simple powder preparation process via polyester polymeric precursors which consist of citric acid and ethylene glycol and this process has been used extensively to produce mixed-cation oxide powders. Recently, some other polymers, such as PVA(polyvinyl alcohol) [10], PEG(polyethylene glycol) [11], PAA(polyacrylic acid) [12–14] and starch-derived polymer [15] have been employed in the preparation of some metal oxides. PVA is water soluble and has many oxygen atoms which have non-bonding electron pairs for combination with metal ions. The use of PVA greatly suppresses the formation of precipitates from which the heterogeneity stems. Thereby, homogeneity in the composition of the precursor can be attained, and thus eliminate the diffusion barrier. It is speculated that the hydroxy ligands on the PVA wrap the metal ions and forming ‘cocoons’ of local structure around the ions, see Fig. 1. This local isolation prevents agglomeration of metal components which inhibits the formation of precipitates. Presumably, this isolation will be

* Corresponding author. Tel.: +82-2-3290-3128; Fax: +82-2-928-7387

0378-7753/99/$ - see front matter
PII: S0378-7753(99)00251-7

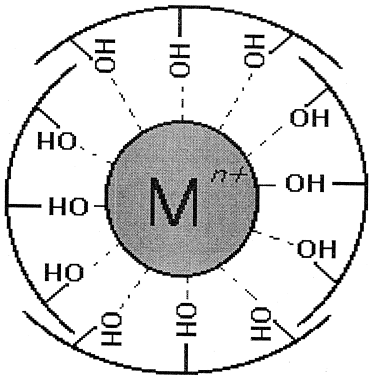

Fig. 1. Cocoon-like local structure around metal ions.

conserved until the organic moieties are burned off during heat treatment. Thus, the PVA-assisted sol–gel method is useful in producing metal oxides with large surface area at low temperature [16].

In this paper, nickel oxide is coated with stable $LiCoO_2$ in carbonate by a PVA-assisted sol–gel method to produce a LC-NiO cathode. The properties of the LC-NiO cathode are monitored during use of the electrode.

2. Experimental

2.1. Preparation of LC-NiO cathode

LC-NiO cathodes were prepared according to the procedure outlined in Fig. 2. At first, lithium acetate ($CH_3COOLi \cdot 2H_2O$, Junsei, EP) and cobalt acetate ($Co(CH_3COO)_2 \cdot 4H_2O$, Junsei, EP) were dissolved in distilled water, stoichiometrically. Another solution was prepared by dissolving polyvinyl alcohol (PVA, degree of polymerization 1500, Yakuri, EP), a chelating agent, in distilled water with mechanical stirring. The molar ratio of PVA to total metal ions was 6. While the PVA solution was constantly stirred, the metal acetate solution was well mixed with the polymer solution, which generated a red transparent solution. The mixed solution was heated at 70 to 80°C. As the evaporation of water proceeded, the solution turned viscous. The porous nickel electrodes were prepared by means of the following procedure. The nickel green sheets were fabricated by a tape-casting method and then sintering was performed at 700°C for 30 min in the reduction atmosphere. The porous nickel electrodes were dipped in the viscous Li/Co-PVA solution for 24 h. After the electrodes were dried at 120°C for 24 h, they were sintered at 650°C for 10 h. The nickel oxide electrodes were coated with a maximum amount of Li/Co-PVA solution; this pre-treatment process was repeated seven or eight times.

2.2. Instrumentation

Thermogravimetric analysis (TGA) and differential scanning calorimetry (DSC) were performed on the Li/Co-PVA sol, the LC-NiO cathode and the pure Ni cathode. Thermal analysis was monitored in an air atmo-

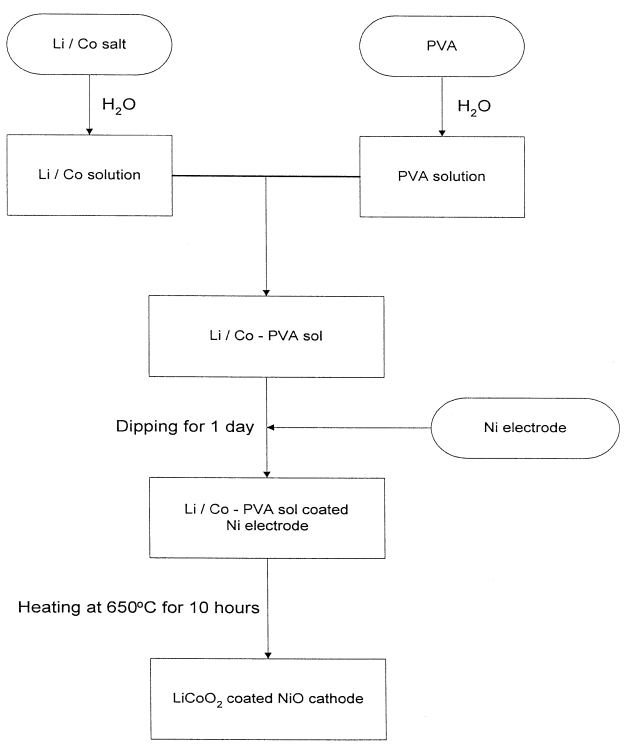

Fig. 2. Fabrication process of LC-NiO cathode.

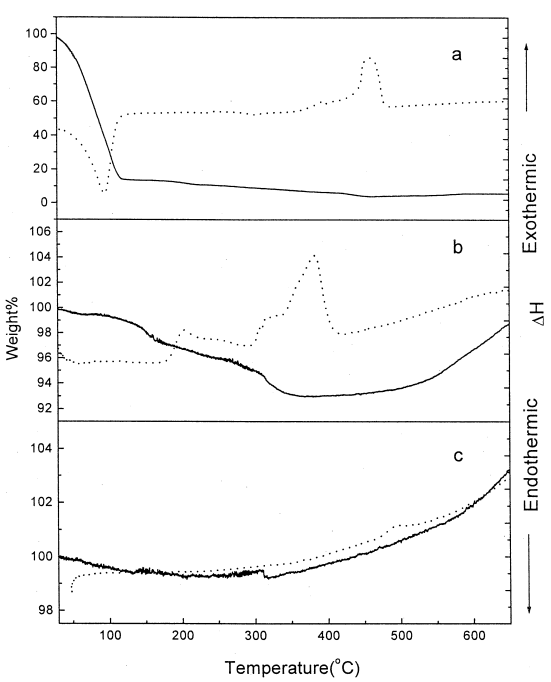

Fig. 3. TGA and DSC curves of (a) Li/Co-PVA sol, (b) LC-NiO cathode, (c) pure Ni cathode.

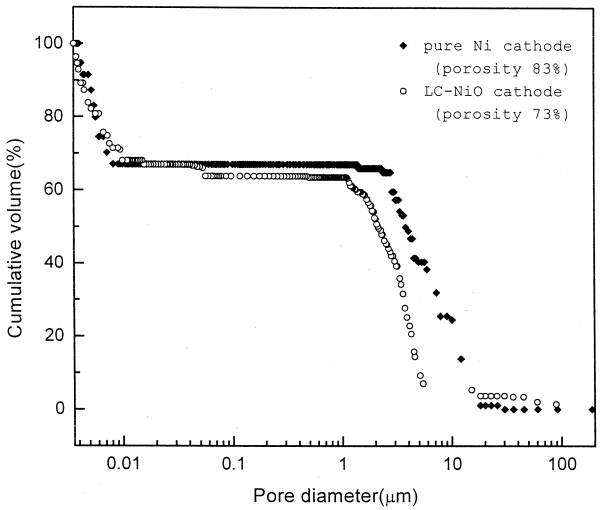

Fig. 4. Plot of pore diameter vs. cumulative volume of various electrodes.

sphere from 30 to 650°C at a heating rate of 10°C/min with Stanton Redcroft TG1000 and Stanton Redcroft DSC1500 equipment. Porosimetry (Micromeritic 9220) was used to measure the pore-size distribution of the various electrodes. A standard test method applied Archimedes' principle to for density and the porosity of sintered powder was used to monitor the porosity of electrodes. This test method is specified by the ASTM Committee B-9 on Metal Powders and Metal Powder Products. The surface structures of the various electrodes were examined by means of scanning electron microscopy (SEM, JEOL JXA-8600), X-ray diffraction (XRD, MAC Science MXP3A-HF), and Raman spectrometry. The XRD patterns of the samples were taken at a scan rate of 4°/min using CuKα radiation. A Model NR-1100 Raman spectrometer from Jasco was used, and the laser source was a Coherent Innova 70 series argon ion laser.

2.3. Unit cell test and solubility test

In order to compare the efficiency of a cell using a NiO cathode with that using a LC-NiO cathode, tests were performed on a 1×1 cm^2 unit cell. A Ni electrode was used and the electrolyte melted at the operating temperature and was then absorbed into a $LiAlO_2$ matrix by the capillary effect. The anode gas component was $68\%H_2/12\%CO_2/20\%H_2O$ and the cathode gas component was $33\%O_2/67\%CO_2$.

The solubility of the LC-NiO cathode was measured in Li_2CO_3/K_2CO_3 (62/38 m/o) eutectic melt. Li_2CO_3 and K_2CO_3 were supplied by the Junsei Chemical and were of analytical purity (> 98%). The melt was purified by a method reported previously and the same experimental apparatus for NiO solubility measurement was used [17]. A 1.5 g LC-NiO cathode was immersed in carbonate melt in an alumina crucible and then the temperature was increased from ambient to 650°C at a rate of 3°C/min. The inlet gas was a mixture of $P_{CO_2} = 0.7$ atm and $P_{O_2} = 0.3$ atm and was supplied at 650°C. Equilibrium solubilities were determined by removing a ~0.3 g aliquot of molten carbonate from the melts at the appointed time using an alumina pipette. Each liquid carbonate sample was transferred to a clean alumina crucible where it solidified. The samples were analyzed for dissolved nickel by inductively coupled plasma (ICP, JOBIN YVON 138 VLTRACE ICP-AES spectrometer).

3. Results and discussion

TGA and DSC curves for the Li/Co-PVA sol, the LC-NiO cathode and the pure nickel cathode are given in Fig. 3. The Li/Co-PVA sol shows a large weight loss and an endothermic reaction curve between 50 and 150°C due to water evaporation. The LC-NiO cathode and the pure nickel cathode show various stepped weight losses and exothermic reaction curves between 300 and 500°C because of the combustion of PVA and organic residues in the electrode. In case of the LC-NiO cathode, the combustion temperature of PVA and organic residues is shifted to a lower value. This means that metal components promote the combustion of PVA, which is the main combustion material [18]. According to the TGA curves of Fig. 3(b) and (c), both electrodes show and increase in weight above 400°C due to the oxidation of nickel.

The pore size distributions of the pure nickel cathode and the LC-NiO cathode are given in Fig. 4. The pure nickel cathode was obtained after the green sheet made by the tape casting method was sintered at 700°C for 30 min in a reduction atmosphere. Both the pure nickel cathode and the LC-NiO cathode exhibit a dual-pore structure which has macro pores (≥ 1 μm) and micro pores (≤ 1

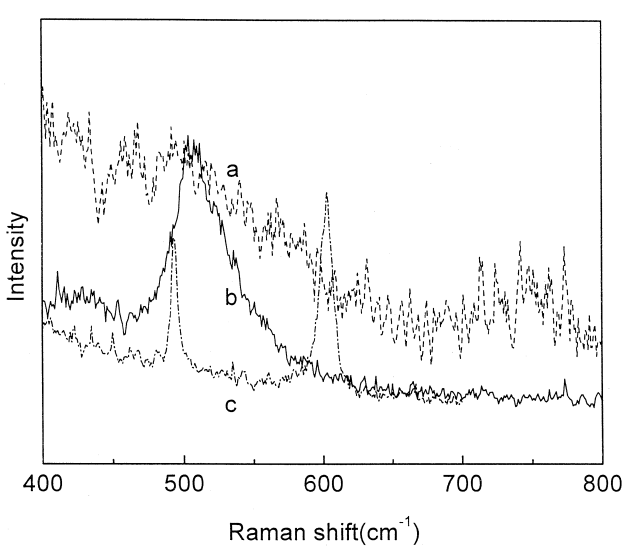

Fig. 5. Raman spectra of (a) NiO cathode, (b) LC-NiO cathode, (c) $LiCoO_2$ powder.

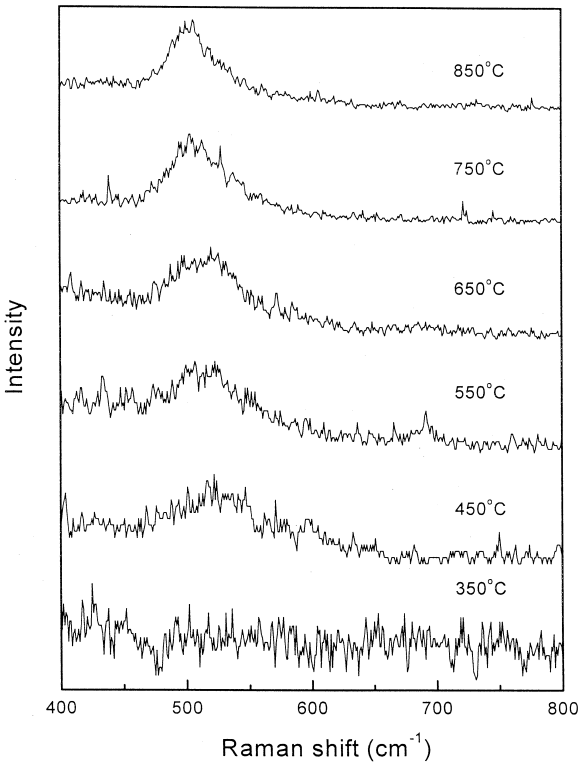

Fig. 6. Raman spectra of a LC-NiO cathode obtained after heat treatment at various temperatures.

μm). This dual pore structure is suitable for a MCFC cathode because the macro pores serve as gas channels for the fuel cell and the micro pores absorb molten electrolyte by the capillary effect. Thus, the reaction of the MCFC is a ternary phase reaction between the solid phase of the electrodes, the liquid phase of the electrolyte and the gas phase of the reaction gases. Comparison of the pore-size distributions of the pure nickel cathode and the LC-NiO cathode shows that the macro pore size of the pure nickel cathode is 7 to 8 μm but that of the LC-NiO cathode is 4 to 5 μm. The reason is that the pore size of LC-NiO electrode decreases during the sintering procedure at high temperature. Actually, the porosity of NiO cathode obtained after sintering at 650°C for 10 h was found to be 72%. The porosity of pure nickel cathode was about 83% and that of LC-NiO electrode was about 73%. If the decrease of the macro-pore size is due to the sintering procedure, the pore structures of two electrodes are very similar and suggests that the coating thickness of $LiCoO_2$ on NiO electrode is very thin.

The Raman spectra of the NiO cathode, the LC-NiO cathode and the pure $LiCoO_2$ powder are presented in Fig. 5. The NiO cathode was obtained after the nickel cathode was oxidized at 650°C for 10 h and the $LiCoO_2$ powder was commercial material supplied by Seimi Chemical. As can be seen from Fig. 5, the spectrum for $LiCoO_2$ powder has two strong Raman bands at 485 and 597 cm^{-1}. By contrast, the spectrum of the NiO cathode is almost featureless. The Raman spectrum of the LC-NiO cathode is different from that of either $LiCoO_2$ or NiO in that it has only one broad band at 510 cm^{-1}. Inaba et al. [19] assigned the above-mentioned two peaks to A_{1g} and E_g vibrational modes. In the A_{1g} mode, the two oxygen atoms

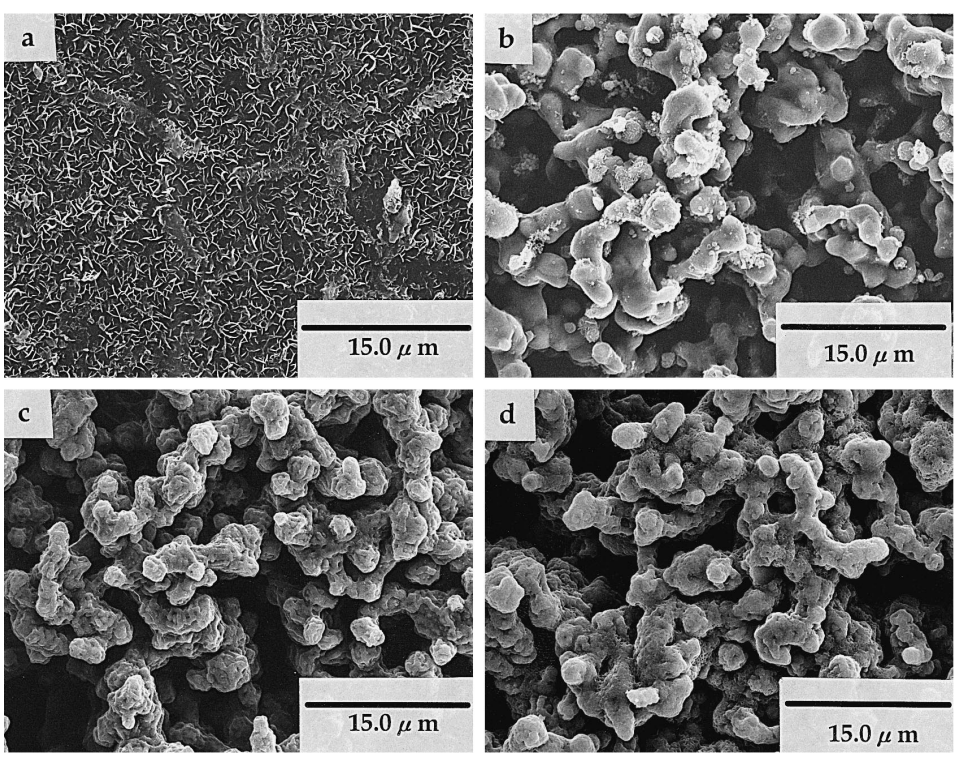

Fig. 7. Electron micrographs of LC-NiO electrodes obtained after heat treatment for 2 h at (a) 350°C, (b) 450°C, (c) 550°C, (d) 650°C.

vibrate in opposite directions parallel to the *c*-axis of $LiCoO_2$, while they vibrate alternately in opposite directions parallel to the Li and Co planes in the E_g mode. The two peaks approach each other and lose their intensities as more Ni replaces Co in $LiCo_{1-y}Ni_yO_2$ $(0 \leq y \leq 1)$. The Raman spectra of the various cathodes which are obtained after heat treatment for 2 h from 350 to 850°C at a hearing rate of 3°C/min are shown in Fig. 6. The data show that the structures of the electrodes which have Li/Co-PVA sol coated on nickel cathodes change to $LiCo_{1-y}Ni_yO_2$ with increase in temperature. The broad Raman band at 510 cm^{-1} for $LiCo_{1-y}Ni_yO_2$ begins to appear at 450°C and its intensity increases with further rise in temperature. From Raman spectra of Figs. 5 and 6, it is found that Li and Co diffuse into the surfaces of the electrodes during the oxidation of nickel above 400°C in the heat-treatment process after electrode dipping. Hence, the surface structure of the LC-NiO cathode obtained after only one pretreatment is $LiCo_{1-y}Ni_yO_2$ formed by Li and Co diffusion into the NiO electrode. A scanning electron micrograph of the electrode obtained after heat treatment at 350°C is given in Fig. 7(a). The Li/Co-PVA film coated on the nickel cathode is observed because the oxidation of organic residue still does not occur at 350°C, as can be seen

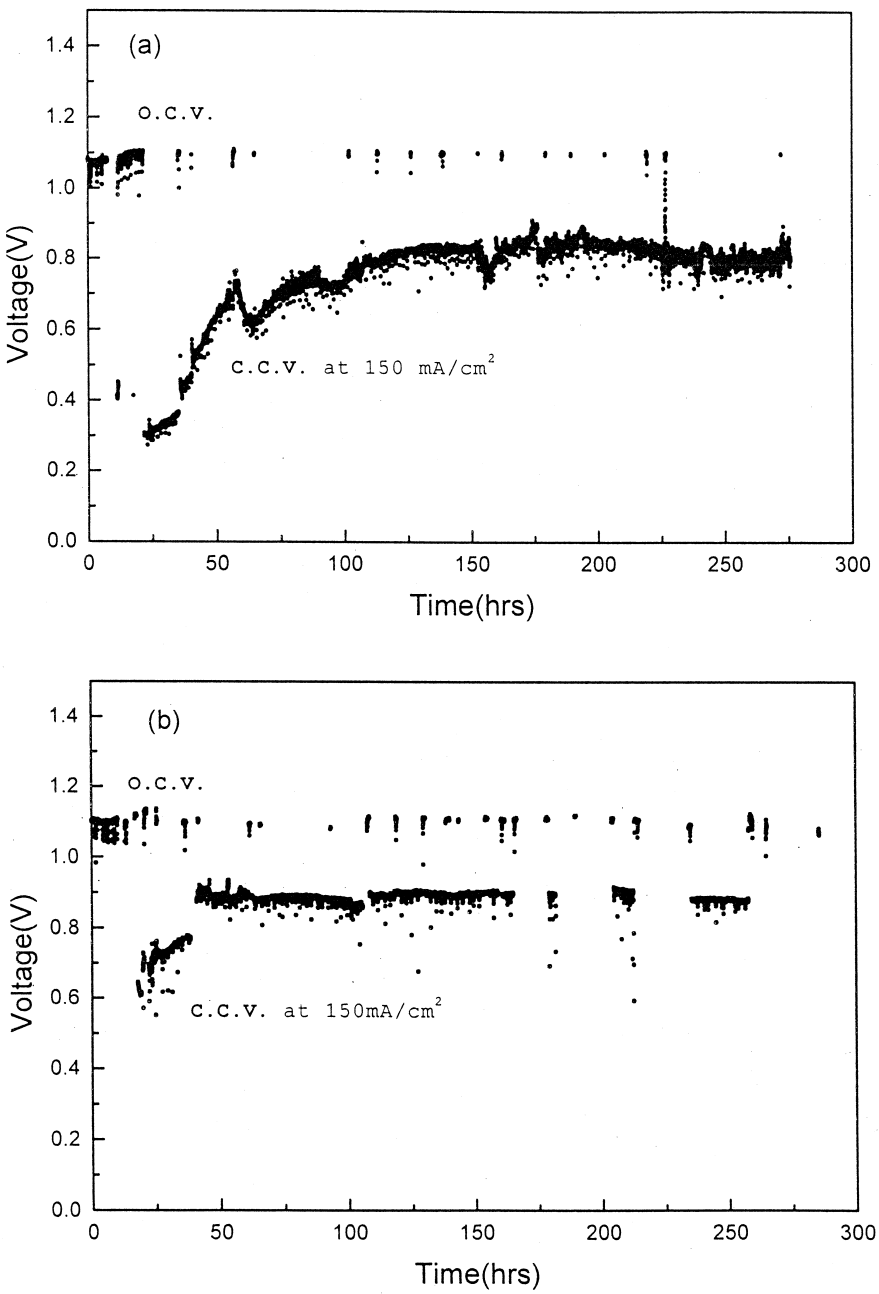

Fig. 8. Unit cell performance using (a) NiO cathode, (b) LC-NiO cathode.

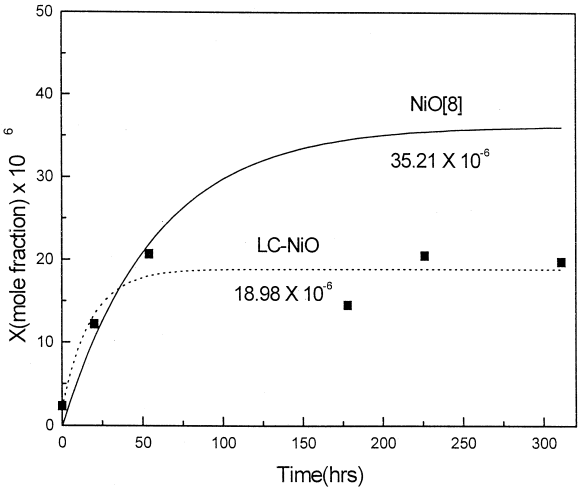

Fig. 9. Solubility of LC-NiO cathode in Li_2CO_3/K_2CO_3 (62/38) melt at 650°C under $P_{CO_2} = 0.7$ atm, $P_{O_2} = 0.3$ atm.

in the TGA and DSC data (Fig. 3). This result is in agreement with the Raman spectrum of the electrode at 350°C (Fig. 6). Because PVA and organic residue is oxidized above 450°C (according to TGA and DSC data), a small amount of organic residue is observed on the surface of NiO cathode. It is not present at 550 and 650°C, due to the completion of organic residue oxidation.

The performance of a 1×1 cm^2 unit cell was evaluated at 650°C for 300 h, and the results are presented in Fig. 8. The open-circuit voltage (OCV) of two unit cells maintained at about 1.1 V and a standard cell consisting of a Ni anode and a NiO cathode showed the closed-circuit voltage (CCV) of ~0.8 V at a current density of 150 mA cm^{-2}. For a unit cell using a LC-NiO cathode, the CCV was ~0.85 V. As can be seen from the results of unit cell performance, the cell using a LC-NiO cathode is superior to that of a cell using NiO. The dissolution curve of a LC-NiO cathode in carbonate melt for $P_{CO_2} = 0.67$ atm and $P_{O_2} = 0.33$ atm at 650°C is shown in Fig. 9. For these conditions, the solubility of LC-NiO cathode is half that of NiO. This behaviour is similar to that shown by a $LiCoO_2$ cathode [8]. Hence, the decrease in solubility of the LC-NiO cathode in a carbonate melt is due to the formation of $LiCo_{1-y}Ni_yO_2$ on the surface of the NiO cathode and this slows the rate of nickel dissolution in the carbonate melt. From the viewpoint of solubility, the LC-NiO cathode might be more stable than the NiO cathode in the carbonate melt.

The XRD patterns of the electrodes obtained after various time pre-treatments are given in Fig. 10. The major XRD peaks for $LiCoO_2$ appear at 19, 37.5, 45.3, 60, 65.6, 66.4° (2θ) [20]. For a LC-NiO cathode obtained after one pre-treatment, the XRD peaks for Ni are observed at 44.5,

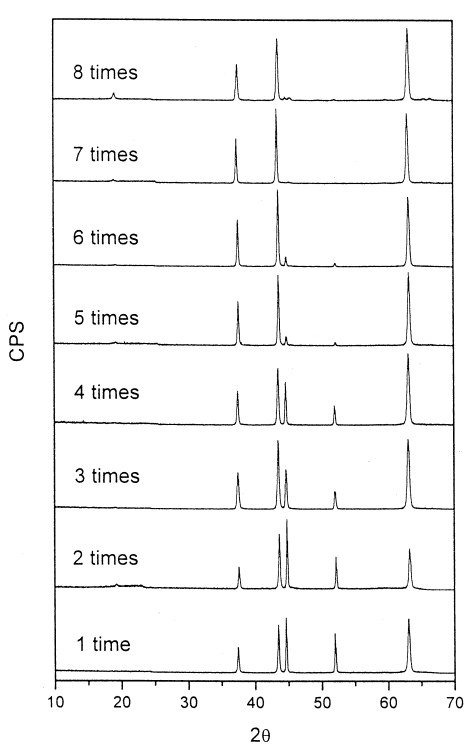

Fig. 10. XRD patterns of LC-NiO cathodes obtained after various pre-treatments.

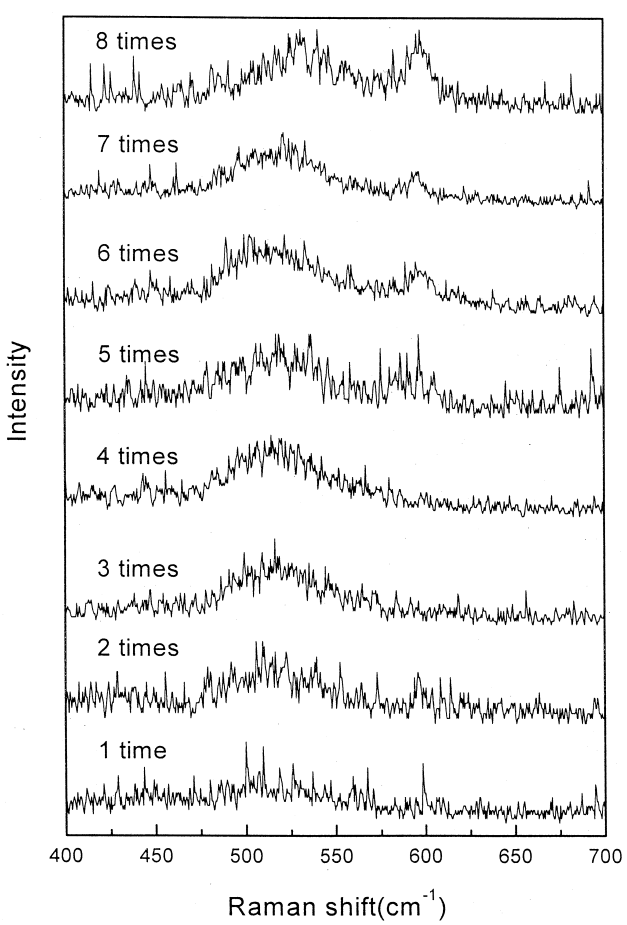

Fig. 11. Raman spectra of LC-NiO cathodes obtained after various pre-treatments.

51.94° [21], and for NiO at 37.3, 43.3, 62.91 and 62.97° [22]. Because of the oxidation of Ni with increase in the pre-treatment time, the intensities of the XRD peaks for Ni decrease and that for NiO increase. The electrode obtained after pre-treatment does not exhibit the major XRD peaks for $LiCoO_2$, whereas the XRD peak for $LiCoO_2$ at 19°(003) appears for an electrode subjected to two pre-treatments. All of the major XRD peaks for $LiCoO_2$ develop for an electrode obtained after seven pre-treatments and appear clearly for a LC-NiO cathode obtained after eight time pre-treatments. The Raman spectra of LC-NiO electrodes obtained after various pre-treatments are shown in Fig. 11. The data are very similar to those obtained from XRD. The LC-NiO cathodes subjected to one to four pre-treatments have a broad band at 510 cm^{-1}, whereas LC-NiO cathodes pre-treated above five times have a Raman band at 597 cm^{-1}. Raman bands for $LiCoO_2$ are observed for a LC-NiO cathode obtained after eight pre-treatments. As can be seen in Figs. 10 and 11, the surfaces of LC-NiO cathodes obtained after a few pre-treatments do not display the $LiCoO_2$ structure in the XRD and Raman data due to the absence of $LiCoO_2$ single crystals. With increase in pre-treatment time, the $LiCoO_2$ structure appears in both the XRD patterns and the Raman spectra because of the formation of $LiCoO_2$ single crystals on the NiO cathode.

4. Conclusions

A new type of cathode (LC-NiO) has been fabricated by a PVA-assisted sol–gel method. Measurements of the pore-size distribution and the porosity of electrodes after dipping and heat treatment confirms that the coating of the electrodes is very thin. The structure of the electrode after only one application of dipping and heat treatment is $LiNi_{1-y}Co_yO_2$ and this structure begins to be formed at 450°C. $LiCoO_2$ is formed with increasing pre-treatment time and a $LiCoO_2$ coating on a NiO cathode is observed after eight pre-treatments. After 300 h of steady operation of unit cells, the mean voltage was 0.80 V for cells using NiO cathodes and 0.85 V for those using LC-NiO cathodes at a current density of 150 mA cm^{-2}. In addition to improving cell efficiency, the LC-NiO cathode has a solubility that is half that of a NiO cathode. Because this new type of cathode is stable in molten salt, it is a promising material for MCFCs.

Acknowledgements

Financial support for this work was given by the Korea Electric Power, and by the Korea Ministry of Education through the Basic Science Research Institute program (1998-015-D00200) and the Center for Mineral Resources (96K3-0503-04-01-4).

References

[1] EPRI, PROC. DOE/EPRI Workshop on MCFCs (EPRI, Palo Alto, CA, 1979), Rep. No. WS-78-135.
[2] J.R. Selman, T.D. Claar (Eds.), Molten carbonate fuel cell technology, Electrochem. Soc., Pennington, NJ, 1982.
[3] K. Kinoshita, F.R. Mc Larnon, E.J. Cairns, Fuel Cells, A Handbook, Chap. 4, DOE/METC-88/6096, 1988.
[4] N.Q. Minh, J. Power Sources 24 (1988) 1.
[5] Molten carbonate fuel cell technology, in: J.R. Selman, D.A. Shores, H.C. Maru, I. Uchida (Eds.), PV 90-16, The Electrochemical Society Softbound Proceeding Series, Pennington, NJ, 1990.
[6] L. Plomp, E.F. Sitters, C. Vessies, F.C. Eckers, J. Electrochem. Soc. 138 (1991) 629.
[7] G.L. Lee, J.R. Selman, L. Plomp, J. Electrochem. Soc. 140 (1993) 390.
[8] K.I. Ota, J. Electrochem. Soc. 142 (10) (1995) 3322–3326.
[9] M.P. Pechini, US Patent No. 3330697, July 11, 1967.
[10] S.K. Saha, A. Pathak, P. Pramanik, J. Mater. Sci. Lett. 14 (1995) 35.
[11] X. Li, H. Zhang, F. Chi, S. Li, B. Xu, M. Zhao, Mater. Sci. Eng. B 18 (1993) 209.
[12] P.A. Lessing, Am. Ceram. Soc. Bull. 68 (1989) 1002.
[13] H. Taguchi, D. Matsuda, M. Nagao, J. Am. Ceram. Soc. 75 (1992) 201.
[14] H. Taguchi, D. Matsuda, M. Nagao, H. Shibahara, J. Mater. Sci. Lett. 12 (1993) 891.
[15] L.-W. Tai, H.U. Anderson, P.A. Lessing, J. Am. Ceram. Soc. 75 (1992) 3490.
[16] H.J. Kwon, S.T. Kuk, H.B. Park, D.G. Park, K. Kim, J. Mater. Sci. Lett. 15 (1996) 428.
[17] K. Ota, S. Mitsushima, S. Kato, S. Asano, H. Yoshitake, N. Kamiya, J. Electrochem. Soc. 139 (1992) 667–671.
[18] H.H. Angermann, F.K. Yang, O. Van der Biest, Int. J. Powder Metall. 28 (1992) 361–367.
[19] M. Inaba et al., Chemistry Letters, 1995, p. 889.
[20] 1994 JCPDS, International Centre for Diffraction Data, 44-0145.
[21] 1994 JCPDS, International Centre for Diffraction Data, 04-0850.
[22] 1994 JCPDS, International Centre for Diffraction Data, 44-1159.